This is a post-peer-review, pre-copyedit version of an article published in *Bulletin of Engineering Geology and the Environment*. The final authenticated version is available online at: https://doi.org/10.1007/s10064-018-1334-2.

Analysis of Schmidt hammer rebound test results with repetitive impacts for determining the mechanical characteristics of weathered pyroclastic rock surfaces: a case study along the Isotake coast, Japan

Tetsuya KOGURE*

Department of Geoscience, Interdisciplinary Graduate School of Science and Engineering, Shimane University, 1060, Nishikawatsu-cho, Matsue, Shimane 690-8504, Japan

*Correspondence to: Department of Geoscience, Interdisciplinary Graduate School of Science and Engineering, Shimane University, 1060, Nishikawatsu-cho, Matsue, Shimane 690-8504, Japan

E-mail address: kogure@riko.shimane-u.ac.jp

Phone: +81-852-32-6445

Fax: +81-852-32-6469

ORCID: 0000-0001-5895-5115

Abstract

Cliffs located along the Isotake coast, Shimane, Japan, are characterized by the development of indents without rockfalls or by the occurrence of rockfalls without indents even though the geology is the same. An analytical method was developed to determine the mechanical properties of the rock surfaces on these coastal cliffs. Twenty continuous impact repetitions of the Schmidt hammer were applied normal to the cliff surfaces in each test. The results of the tests (26 with indents and 22 without indents) showed a gradual increase in the rebound as the number of repetitions increased. A new exponential equation was proposed in this study to describe the features of the weathered surfaces. The changes in the results were well approximated by the equation, and the approximation clearly distinguished between the two types of weathered surfaces, with higher rebound values at the surface of the indents than those at the surface of cliffs without indents. The homogeneity/heterogeneity of the surface and inner body of the cliff rock can also be modelled by coefficients appearing in the equation.

Keywords: Schmidt hammer; repetitive impacts; rhyolitic pyroclastic rocks; exponential equation; coastal cliff; weathering

Introduction

A rockfall accident that caused a human death occurred approximately 60 years ago at a cliff on the Isotake coast of Shimane, Japan. The residents of this area have been aware of the danger of rockfalls, and they have not approached the coastal cliffs since then, because rockfalls are common. Residents insist that the rockfalls occur at cliffs composed of “soft rock” and do not occur at cliffs composed of “hard rock”; however, the descriptions of “soft” and “hard” are not derived from physical or mechanical tests on the rocks but based on their personal opinion. First, the physical or mechanical properties of the cliff material should be evaluated quantitatively to understand the mechanisms of the rockfalls in this area.

In situ measurements, including the Schmidt hammer rebound test (SH test), are appropriate for measuring the mechanical properties of the rock materials because the lithology of the cliff mass is a pyroclastic rock including gravel or boulders that are too large to provide specimens for laboratory tests. The Schmidt hammer, which is a non-destructive apparatus for evaluating the hardness of rock in the laboratory and *in situ*, has been widely used for engineering purposes and in scientific research. The SH test is often used to determine the strength of rocks as an alternative to laboratory testing because the rebound value is closely related to the uniaxial compressive strength (Aydin and Basu 2005). Aydin (2009) states that it determines not only the rebound value at each measurement point but also the degree of weathering of rock materials. Because it is difficult to drill or cut the surface of the cliff due to the hardness of the surface or the risk of rockfalls, the SH test is a good way to evaluate the mechanical properties of the cliff materials in the present study.

The aim of the present study is to determine the mechanical properties of the cliff materials in this area by the SH test. For this purpose, an analytical method is proposed for characterizing weathered surfaces from the results of the SH test.

Geological and geomorphological settings of the study cliff

Sandy beaches and coastal cliffs with heights exceeding 30 m have developed along the coastline at Ohda City, Shimane, Japan (Fig. 1). The Isotake coastline runs ENE-WSW and faces the Sea of Japan to the north. The geology of this area consists mainly of the Miocene Kuri Formation, which is composed of andesitic, dacitic and rhyolitic lava and pyroclastic rocks and mudstone with maximum thicknesses of 700−800 m, and the bedrock is the Paleocene Nojiro Granite (Kano et al. 1998). In the Kuri Formation, the cliffs are composed of rhyolitic pyroclastic rocks. These rocks were erupted during the opening of the Sea of Japan, which occurred mainly during the interval 16.1−14.2 Ma (Otofuji et al. 1991).

The study cliff is located on the Isotake coast (Fig. 1). The maximum height of the cliff is approximately 40 m, and the top surface is covered by vegetation (Fig. 2a). The study cliff has some indents characterized by brown-coloured surfaces in its seaward aspect, although the colour of the entire cliff surface is greyish (Fig. 2a). Some cliffs in this area have similar indents on their vertical surfaces, with maximum heights and breadths exceeding 10 m and a depth of several metres, at least on the seaward aspect. Figure 2a shows some fallen blocks at the base of the study cliff. They must have been derived from the cliff surface just behind them because the surface bears scars from collapse. On the other hand, no fallen blocks exist in front of the largest indent, and the surface of the indent has no scars from collapse (Fig. 2a). Hereafter, a cliff surface with an indent is referred to as Type A, and a cliff surface without indents as Type B. Figure 2b shows the vertical profiles of the study cliff along the dotted lines in Fig. 2a. The profile along Line VA includes an indent, which is a depressed section presented with a bold line.

Type A and Type B both have roughness that is due to the projection of clasts included in the pyroclastic rock. There are some differences in the characteristics of the surfaces, however. The most pronounced difference is in the colour of the surfaces, even though they have the same geology; the colour is brown for Type A, (Fig. 3a) and grey for Type B (Fig. 3b). The petrological characteristics of the rocks from both surfaces were confirmed by the observation of thin sections. Figure 4 shows photomicrographs of the pyroclastic rocks from Types A and B. The photomicrographs reveal that rocks from both surfaces have the same mineral composition. The type of rock at the surfaces is, of course, the same even though the colour of each surface is different.

Brown crystals are precipitated on the surfaces of the indents (Fig. 5a). No brown crystals are found on the surface of the cliffs without indents, however. Therefore, the brown crystals appear to cause the difference in colour between the surfaces. The brown crystals exhibit several shapes: flower-like (Fig. 5a), pillar-like, flattened, and amorphous. The maximum length of the projected crystals is approximately 10 cm. These crystals are easily broken by the impact of a rock hammer. X-ray diffraction analysis (XRD) was conducted to identify the brown crystals. The XRD pattern was recorded by a Rigaku diffractometer (Rint 2000) using CuKα at 30 kV and 20 mA. The analysis was between 2° and 40° at 2θ steps of 0.02 and a scan speed of 2° per minute. Figure 5b shows the XRD pattern of a brown crystal. The pattern obtained in this study was compared to those from the database provided by the RRUFF Project (Lafuente et al., 2015) in order to identify the type of crystal. The analysis shows that the mineral that comprises the brown crystals is calcite (Fig. 5b).

Schmidt hammer rebound test

The hammer used in this study was a GS-type for rocks, made by Sanyo Testing Machines Co., Japan, and is as same as the KS-type from Proceq, having an impact energy of 2.207 Nm. There have been several studies on the multiple impact method for the SH test in order to evaluate the degree of weathering (Basu et al. 2009; Matsukura and Aoki 2004). We followed the continuous (repeated) impact method proposed by Matsukura and Aoki (2004). They explained that repeated impacts at the same point without any release of the hammer from the rock surface generate an understanding of the degree of weathering of the surface and make it possible to assess the hardness of the intact rock. The rebound value increases as the number of repeated impacts increases, because weathered surfaces that are loose become firm due to compacting of the grains. Each test involved 20 impact repetitions.

The SH test was conducted at 26 points for Type A (A1-A26) and 22 points for Type B (B1-B22) surfaces along lines HA and HB (Fig. 2a). The impact of the Schmidt hammer was normal to the vertical surfaces at all the measurement points. Some researchers have proposed that the measured surface should be polished before impact, because the results may be influenced by the surface texture, with smooth planar surfaces giving higher readings than rough or irregular surfaces (Williams and Robinson 1983); also, the magnitude and repeatability of the hammer readings vary depending on the degree of polishing (Katz et al. 2000). In the present study, however, the SH test was performed without any polishing of the surfaces before impact. Various sizes of particles from sand to boulders densely cover the surface of the study cliff (Fig. 3). As a result, it was not possible to render the surface flat and smooth using the carborundum supplied with the instrument. The test points were selected to avoid boulders which would prevent the hammer from impacting the matrix directly. The impacted test points became flatter than those before the continuous impacts for rocks from both Type A and Type B (Fig. 6). The processes causing flattening may include the compacting of a weathered surface, detachment of small particles, and breaking of the matrix. These processes are reflected in the changes in rebound values, especially in the early stage of repetitive impact, which yields lower values than those from an intact rock.

Results and discussion

Approximation of the Schmidt hammer rebound value

Figure 7a shows the relation between the rebound value, R_n, and the number of impacts obtained from the SH test for A12, A25 and B9 (Table 1). These sample points were shown as extreme examples in terms of the scattering of plots: the smallest for B9, the second largest for A25 and the largest for A12. The weathered surface for A12 seems to be very thin because R_n, except for R_1, remains between 50 and 60, which corresponds to the maximum rebound value, R_{max}, at other measurement points (Table 1). The values of R_n increase gradually with increasing numbers of impacts. The value of R_n was obtained for the n-th (n=1-20) impact; Fig. 7a plots R_n against (n-1). The quantitative modelling of the changes in R_n by an equation appears to be useful to characterize both types of weathered surfaces. Considering that R_n appears to converge to a constant value (Aoki and Matsukura (2007); present study), the equation should have an intercept. Furthermore, some studies on weathering rates use exponential expressions to show the changes in the rates which decrease with increasing time (e.g., Matsukura and Matsuoka 1991), which is similar to those in R_n. Therefore, an exponential equation with an intercept is proposed as:

$$R_n = a\left(1 - \exp\left(-b(n-1)\right)\right) + R_1 \quad (1)$$

Here, R_1 is the rebound value measured at the first impact, and *a* and *b* are constants. The constants are calculated by mathematical software in which users can define a type of approximate equation (KaleidaGraph by Synergy Software Inc. was used in this study). Equation (1) was used to model all data from the SH test. Table 1 lists the values of *a* and *b* obtained using Eq. (1), except for A12, which was not suitable because of the large scattering in the plots (Fig. 7a). Figure 7a shows an example of this curve-fitting with the highest and lowest values of the coefficient of determination, R^2, which are 0.98 for B9 and 0.50 for A25.

Surface conditions of the study cliff

The values of R^2 were generally higher for B1-B22 than for A1-A26 (Table 1); the mean values were 0.91 (standard deviation: 0.061) for B1-B22, and 0.81 (standard deviation: 0.096) for A1-A26. These results indicate that the Type B cliff surfaces are more homogeneous than the Type A surfaces. If there is a large deformation of the surface or exfoliation of surface material, such features may prevent the hammer from making consistent impacts with the surface. The lower value of R^2 for Type A suggests that this problem is more common for Type A.

Figure 7b shows the relation between the minimum rebound value, R_{min}, and R_{max}, as obtained from the plots of R_n-change for each impact point; an example is shown in Fig. 7a for B9. At every impact point, R_1 corresponds to R_{min}. The open and filled circles show the data from A1-A26 and B1-B22, respectively. The open and filled circles appear in different areas. The values of R_{min} for A1-A26 vary from 13 to 36, and they vary for B1-B22 from 12 to 18. The scatter in R_{min} is larger for A1-A26 than for B1-B22. However, the tendency in the scatter for R_{max} is different from that for R_{min}. The values of R_{max} for A1-A26 vary from 54 to 63, and they vary for B1-B22 from 28 to 48. The relation between R_{min} and R_{max} for A1-A26 and B1-B22 therefore has certain characteristics: “horizontal scattering” for A1-A26 and “vertical scattering” for B1-B22. Here, “horizontal scattering” means that changes in R_{min} are large compared to those in R_{max} and conversely for “vertical scattering”. On the basis of these patterns, surface conditions are estimated as follows: (1) the inner body of Type A is homogeneous, whereas the surface condition is heterogeneous and (2) the inner body of Type B is heterogeneous whereas the surface condition is homogeneous (Table 2). Studying the changes in petrological/mineralogical features (e.g., statistics for clast sizes, shapes, roundness, matrix properties, and minerals) and physical/mechanical properties (e.g., porosity, density, and strength) from the surface to the inner body before and after the SH test reveals more details about the nature of the rebound values.

Figure 8 shows the relation between the results of the SH test and the exponential model, Eq. (1). The constants a and b have the physical interpretation that a affects the magnitude of R_n and b controls the rate of change of R_n. Figure 8a shows the relation between the constants a and b. The value of a for A1-A26 varies from 19.3 to 42.0, and for B1-B22 from 12.4 to 30.9, while the value of b has almost identical ranges for Type A and Type B. The similar ranges for *b* indicate that the numbers of impacts required for R_n to converge are similar in Type A and Type B.

A good correlation was found between the ratio of R_{max} to R_{min} (R_{max}/R_{min}) and the constant *a* (Fig. 8b). The values of R_{max}/R_{min} and *a* may both reflect the difference in rebound values of weathered surface and compressed weathered surface (or intact inner body if the weathered surface is relatively thin), because R_n is initially lower for a weathered surface but then increases as the surface becomes denser and more consolidated due to the repeated hammer impacts. In Fig. 8b, the value of *a* for A1-A26 is higher than that for B1-B22 at the same value of R_{max}/R_{min}. These plots clearly distinguish the characteristics of the changes in R_n for the two distinct types of weathered surface. Two linear trend lines are shown in Fig. 8b, relating to the plots for A1-A26 and B1-B22. Of the data for Type A, A3, A13, A14, A16 and A24 are plotted around the line for B1-B22. They have R_{min} values of 13-15, which are in the range of R_{min} variation for B1-B22, i.e., 12-18. The values are significantly smaller than the mean value of R_{min} for A1-A26 (Table 1). This result may be due to high surface roughness. The value of R_1 is small if the first impact is upon particles that are easily removed. The plots of A3, A13, A14, A16 and A24 consequently move leftward, to be plotted around the other line when the SH test is conducted at a smoother surface where the value of R_{max}/R_{min} is small.

The results of the repeated SH test and its successful modelling by an exponential equation proved useful in distinguishing the surface conditions of Type A and Type B (Table 2). The surfaces of Type

A and Type B consist of weathered rock with a loose matrix and become consolidated due to the compacting effects of the repeated impacts. The repeated SH test is capable of detecting the difference in characteristics of the two kinds of weathered surface conditions, as manifest in the changes in R_n.

Conclusions

The Schmidt hammer rebound test was conducted in order to determine the mechanical properties of the weathered surface of a cliff on the Isotake coast of Shimane, Japan, as the first step to understand the rockfall mechanism for the cliff. Approximating the results of the Schmidt hammer rebound test by the exponential equation proposed in this study clearly distinguished two types of weathered surfaces, with higher rebound values at the surface of the indents than those at the surface of cliffs without indents.

The analysis of the results of the Schmidt hammer test in this study can be applied to any type of rock surface. Data from different types of rock with differing degrees of weathering will improve this method and provide better future estimates of the characteristics of weathering as determined by the Schmidt hammer test.

Acknowledgements

The author appreciates Dr. Hiroto Ohira in Shimane University for technical support on XRD analysis. This study was supported partly by JSPS KAKENHI Grant Number 15H05350 through TK. This is a post-peer-

review, pre-copyedit version of an article published in *Bulletin of Engineering Geology and the Environment*. The final authenticated version is available online at: https://doi.org/10.1007/s10064-018-1334-2.

References

Aoki H, Matsukura Y (2007) A new technique for non-destructive field measurement of rock-surface strength: an application of the Equotip hardness tester to weathering studies. Earth Surf Process Landf 32:1759–1769. doi:10.1002/esp.1492

Aydin A (2009) ISRM Suggested method for determination of the Schmidt hammer rebound hardness: Revised version. Int J Rock Mech Min Sci 46:627–634. doi:10.1016/j.ijrmms.2008.01.020

Aydin A, Basu A (2005) The Schmidt hammer in rock material characterization. Eng Geol 81:1–14. doi:10.1016/j.enggeo.2005.06.006

Basu A, Celestino TB, Bortolucci AA (2009) Evaluation of rock mechanical behaviors under uniaxial compression with reference to assessed weathering grades. Rock Mech Rock Eng 42:73–93. doi:10.1007/s00603-008-0170-2

Kano K, Matsuura H, Sawada Y, Takeuchi K (1998) Geology of the Iawami-Ōda and Ōura Districts with geological sheetmap at 1:50000. Geological Survey of Japan, Tsukuba (in Japanese with English abstract).

Katz O, Reches Z, Roegiers J-C (2000) Evaluation of mechanical rock properties using a Schmidt Hammer. Int J Rock Mech Min Sci 37:723–728. doi:10.1016/S1365-1609(00)00004-6

Lafuente B, Downs RT, Yang H, Stone N (2015) The power of databases: the RRUFF project. In: Armbruster T, Danisi RM (eds) Highlights in Mineralogical Crystallography, Walterde Gruyter, Berlin (http://rruff.info/about/downloads/HMC1-30.pdf)

Matsukura Y, Aoki H (2004) The Schmidt hammer: a brief review and some problems in geomorphology. *Trans Jpn Geomorph Union* 25:175–196 (in Japanese with English abstract)

Matsukura Y, Matsuoka N (1991) Rates of tafoni weathering on uplifted shore platforms in Nojima-Zaki, Boso Peninsula, Japan. Earth Surf Process Landf 16:51–56. doi:10.1002/esp.3290160106

Otofuji Y, Itaya T, Matsuda T (1991) Rapid rotation of southwest Japan - paleomagnetism and K-Ar ages of Miocene volcanic-rocks of Southwest Japan. Geophys J Int 105:397–405. doi:10.1111/j.1365-246X.1991.tb06721.x

Williams RBG, Robinson DA (1983) The effect of surface texture on the determination of the surface hardness of rock using the Schmidt Hammer. Earth Surf Process Landf 8:289–292. doi:10.1002/esp.3290080311

Captions

Table 1 Results of the Schmidt hammer test

Table 2 Summary of the characteristics of cliff surfaces in terms of the Schmidt hammer rebound values

Fig. 1 Location of the study cliff. The cliff is included in an area of distinct relief indicated by an arrow

Fig. 2 Study cliff: (a) vertical surfaces of the study cliff with indents on the seaward part and rockfalls on the inland side and (b) vertical profiles of the study cliff, with indents along Lines VA and VB in Fig. 2a. The picture was taken from the west

Fig. 3 Close-up photos of cliff surfaces: (a) Type A and (b) Type B

Fig. 4 Photomicrographs of pyroclastic rocks from Type A and Type B. The abbreviations “Pl” and “Qtz” denote plagioclase and quartz, respectively

Fig. 5 Brown crystal on the surface of an indent: (a) photograph and (b) XRD pattern

Fig. 6 Close-up photos of the SH test points after impacts for (a) Type A and (b) Type B

Fig. 7 Results of the Schmidt hammer rebound test using the repeat method. (a) Examples of changes in R_n for Type A and Type B. Of the data, A25 and B9 have the smallest and largest coefficients of determination, R^2: 0.50 for A25 and 0.98 for B9. A12 exhibits greater scattering and is not suitable for approximation by Eq. (1). (b) The relation between $R_{\max}$ and $R_{\min}$. The plots for A1-A26 and B1-B22 show “horizontal scattering” and “vertical scattering”, respectively

Fig. 8 Relations between parameters estimated from the model of Eq. (1). (a) Relation between *a* and *b* in Eq. (1). (b) Relation between R_{max}/R_{min} and *a*. The plots for A1-A26 and B1-B22 are clearly distinguished, although some data from Type A with smaller R_{min} are plotted at the extension of B1-B22

Table 1

No.	R_{max}	R_{min}	R_{max}/R_{min}	a	b	R^2	No.	R_{max}	R_{min}	R_{max}/R_{min}	a	b	R^2
A1	60	36	1.67	19.3	0.54	0.61	B1	36	12	3.00	22.2	0.42	0.88
A2	62	19	3.26	38.3	0.29	0.83	B2	41	14	2.93	23.9	0.47	0.91
A3	58	13	4.46	39.4	0.68	0.75	B3	42	16	2.63	24.9	0.19	0.94
A4	61	27	2.26	28.9	0.56	0.80	B4	40	16	2.50	22.4	0.32	0.96
A5	54	30	1.80	20.7	0.46	0.82	B5	48	16	3.00	28.6	0.62	0.92
A6	60	23	2.61	33.9	0.37	0.89	B6	38	12	3.17	21.8	0.57	0.89
A7	56	25	2.24	27.6	0.31	0.81	B7	48	14	3.43	30.9	0.45	0.94
A8	59	24	2.46	29.5	0.69	0.80	B8	40	17	2.35	21.4	0.72	0.96
A9	59	35	1.69	20.7	0.63	0.85	B9	34	15	2.27	18.0	0.28	0.98
A10	54	27	2.00	21.7	0.64	0.78	B10	35	12	2.92	23.0	0.21	0.96
A11	59	25	2.36	30.6	0.44	0.90	B11	41	18	2.28	21.2	0.27	0.84
A12	60	31	1.94	-	-	-	B12	37	12	3.08	22.4	0.35	0.93
A13	62	15	4.13	42.0	0.45	0.88	B13	38	18	2.11	18.9	0.71	0.97
A14	55	15	3.67	35.3	0.36	0.78	B14	42	13	3.23	27.2	0.75	0.96
A15	62	29	2.14	27.6	0.84	0.78	B15	40	18	2.22	20.2	0.31	0.91
A16	59	14	4.21	39.9	0.58	0.89	B16	34	17	2.00	15.2	0.31	0.90
A17	62	28	2.21	32.2	0.18	0.71	B17	36	14	2.57	19.6	0.58	0.85
A18	63	28	2.25	30.4	0.43	0.87	B18	30	12	2.50	15.1	0.42	0.72
A19	61	28	2.18	27.8	0.80	0.70	B19	28	15	1.87	12.4	0.26	0.86
A20	58	26	2.23	32.9	0.15	0.85	B20	33	14	2.36	17.8	0.31	0.95
A21	62	28	2.21	30.5	0.45	0.84	B21	31	14	2.21	15.0	0.51	0.83
A22	60	23	2.61	33.5	0.88	0.85	B22	37	16	2.31	19.5	0.77	0.91
A23	58	21	2.76	34.2	0.49	0.90							
A24	57	14	4.07	37.6	0.52	0.86							
A25	56	30	1.87	20.4	0.26	0.50							
A26	57	20	2.85	33.8	0.73	0.92							
A1-A26 M.V.*	59.0	24.4	2.60	30.7	0.51	0.81	B1-B22 M.V.*	37.7	14.8	2.59	21.0	0.45	0.91
A1-A26 S.D.**	2.6	6.4	0.83	6.5	0.20	0.096	B1-B22 S.D.**	5.1	2.1	0.44	4.6	0.18	0.061

*M.V. stands for mean value

**S.D. stands for standard deviation

Table 2

Cliff surface	Rebound value		Estimated condition	
	R_{max}	R_{min}	Inner body	Surface
Type A	54-63	13-36	Intact and homogeneous	Heterogeneous
Type B	28-48	12-18	Not intact and heterogeneous	Not intact and homogeneous

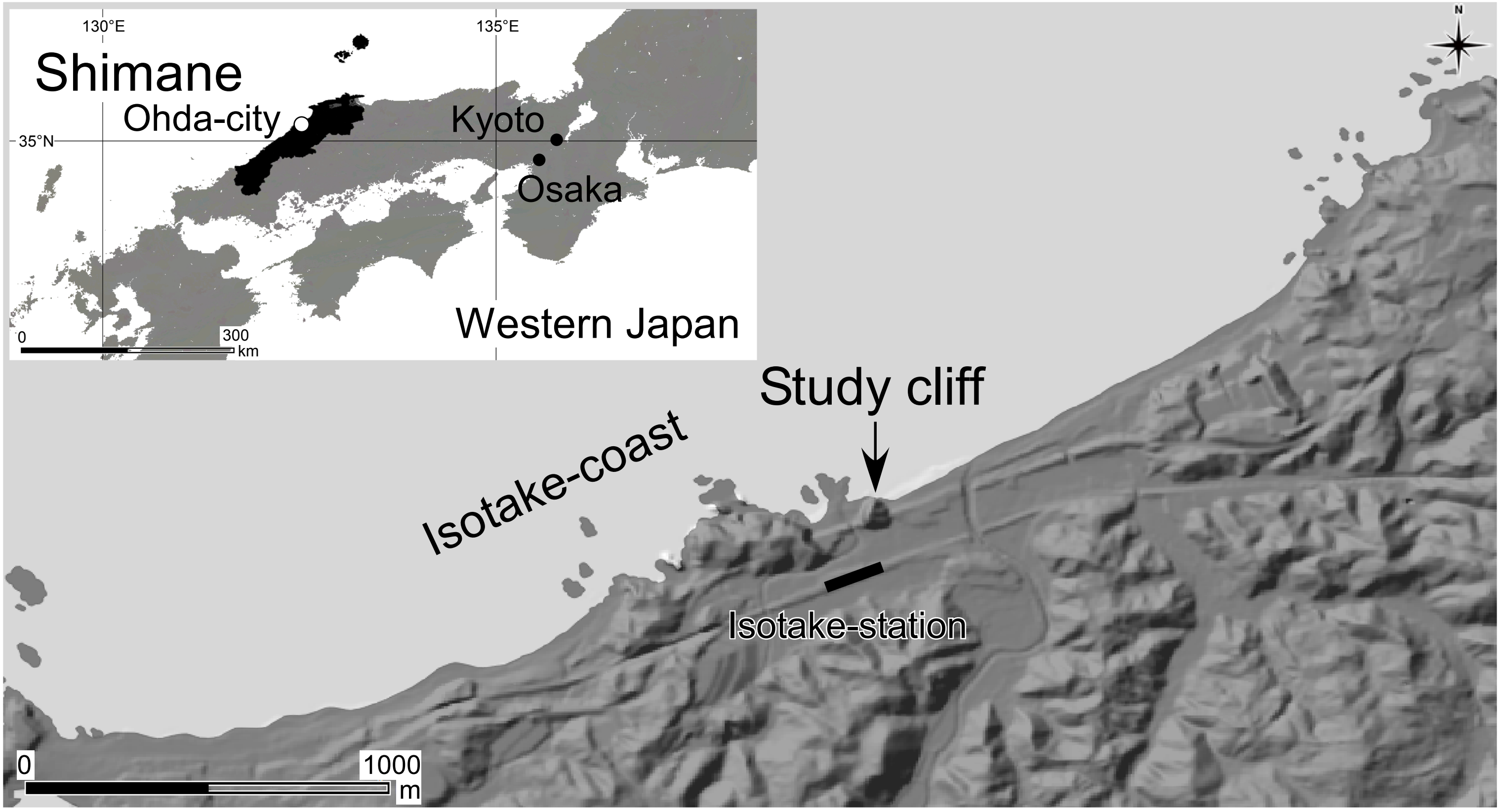
130°E
135°E
Shimane
Ohda-city
Kyoto
35°N
Osaka
0
300
km
Western Japan
N
Study cliff
Isotake-coast
Isotake-station
0
1000
m

Figure 1

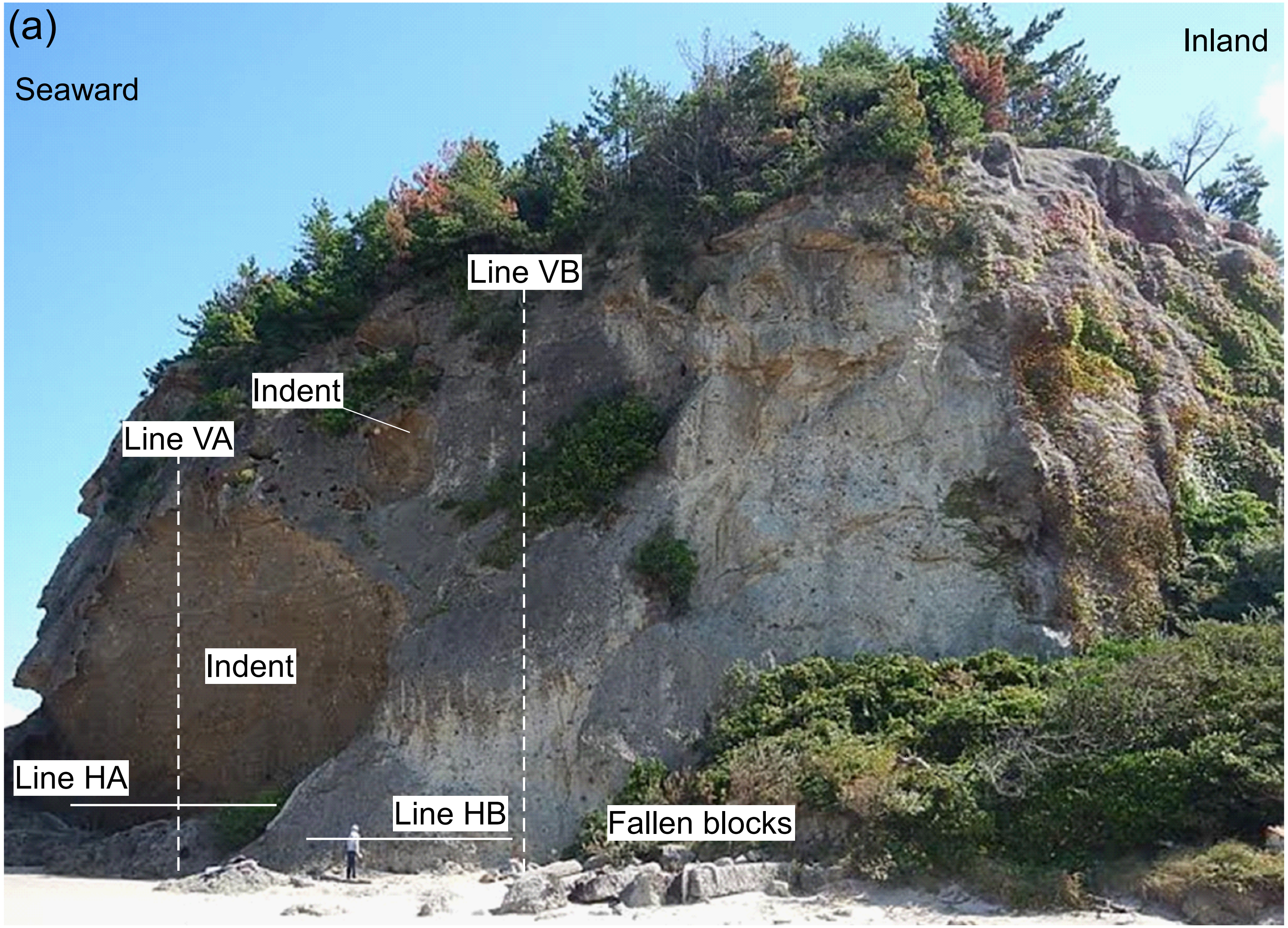
(a)
Seaward
Inland
Line VB
Indent
Line VA
Indent
Line HA
Line HB
Fallen blocks

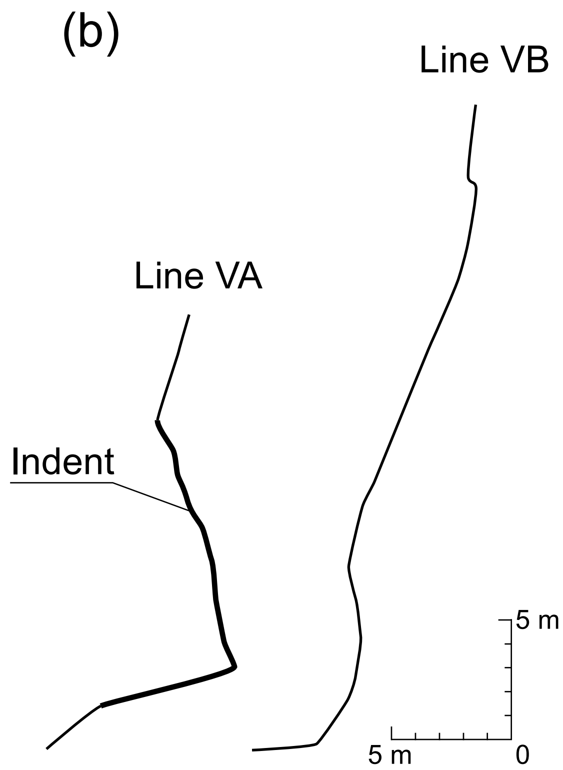
(b)
Line VB
Line VA
Indent
5 m
5 m
0

Figure 2

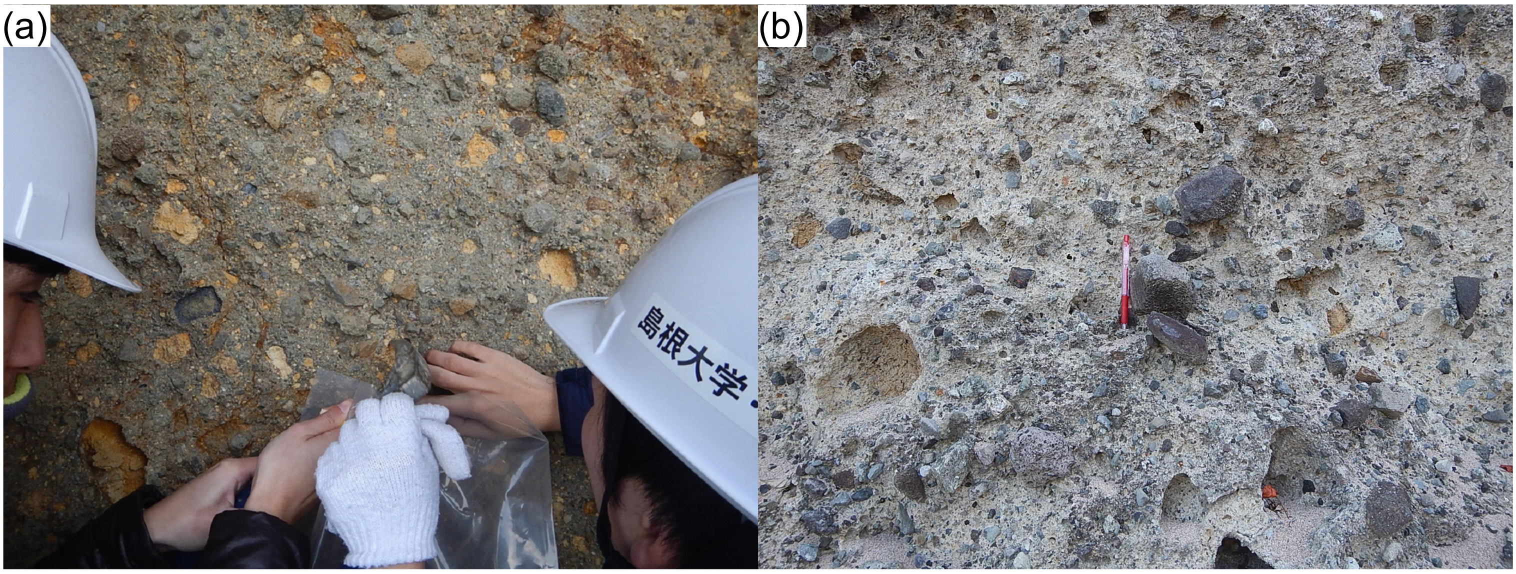

Figure 3

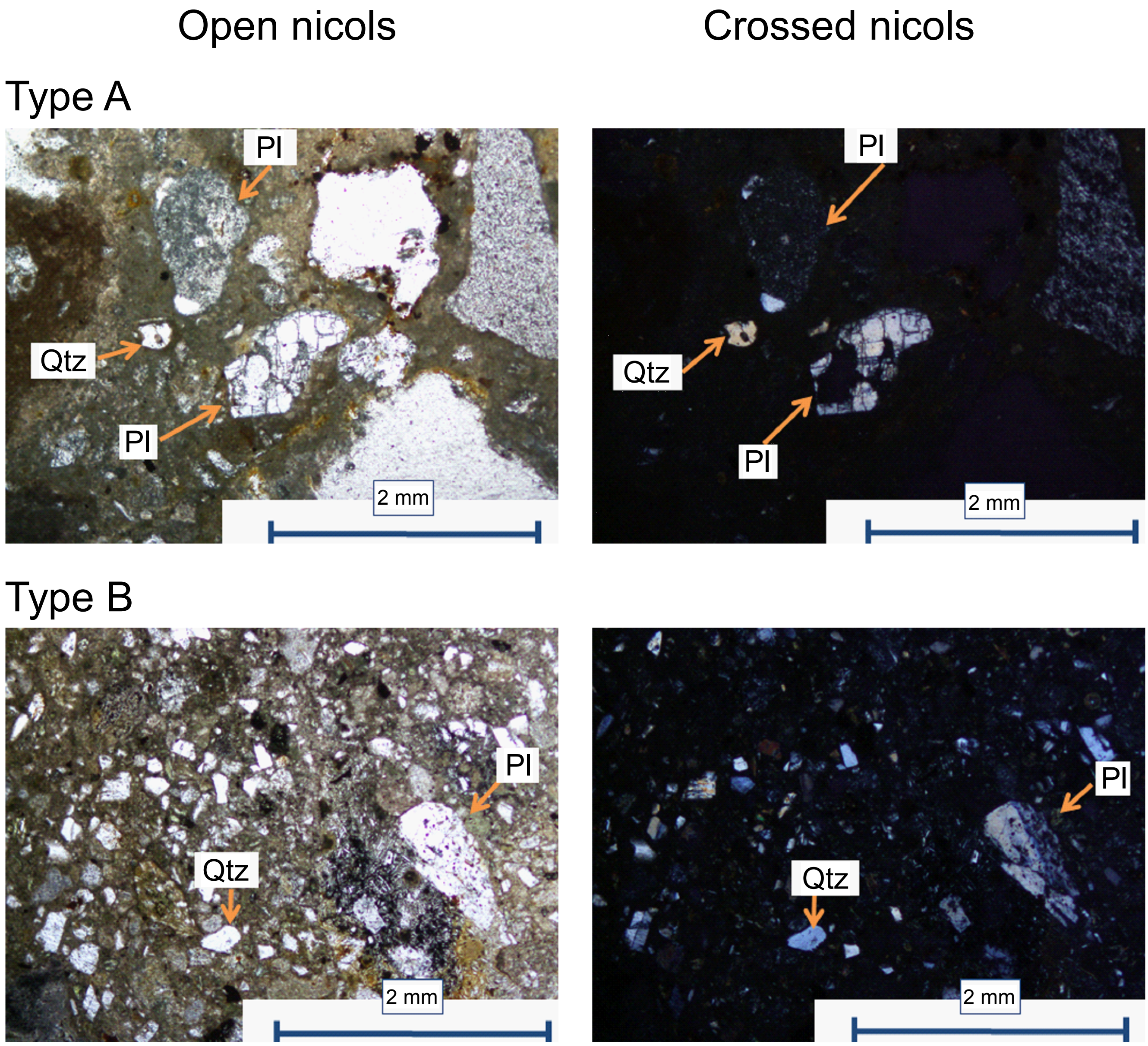

Open nicols
Crossed nicols
Type A
Pl
Qtz
Pl
2 mm
Pl
Qtz
Pl
2 mm
Type B
Pl
Qtz
2 mm
Pl
Qtz
2 mm

Figure 4

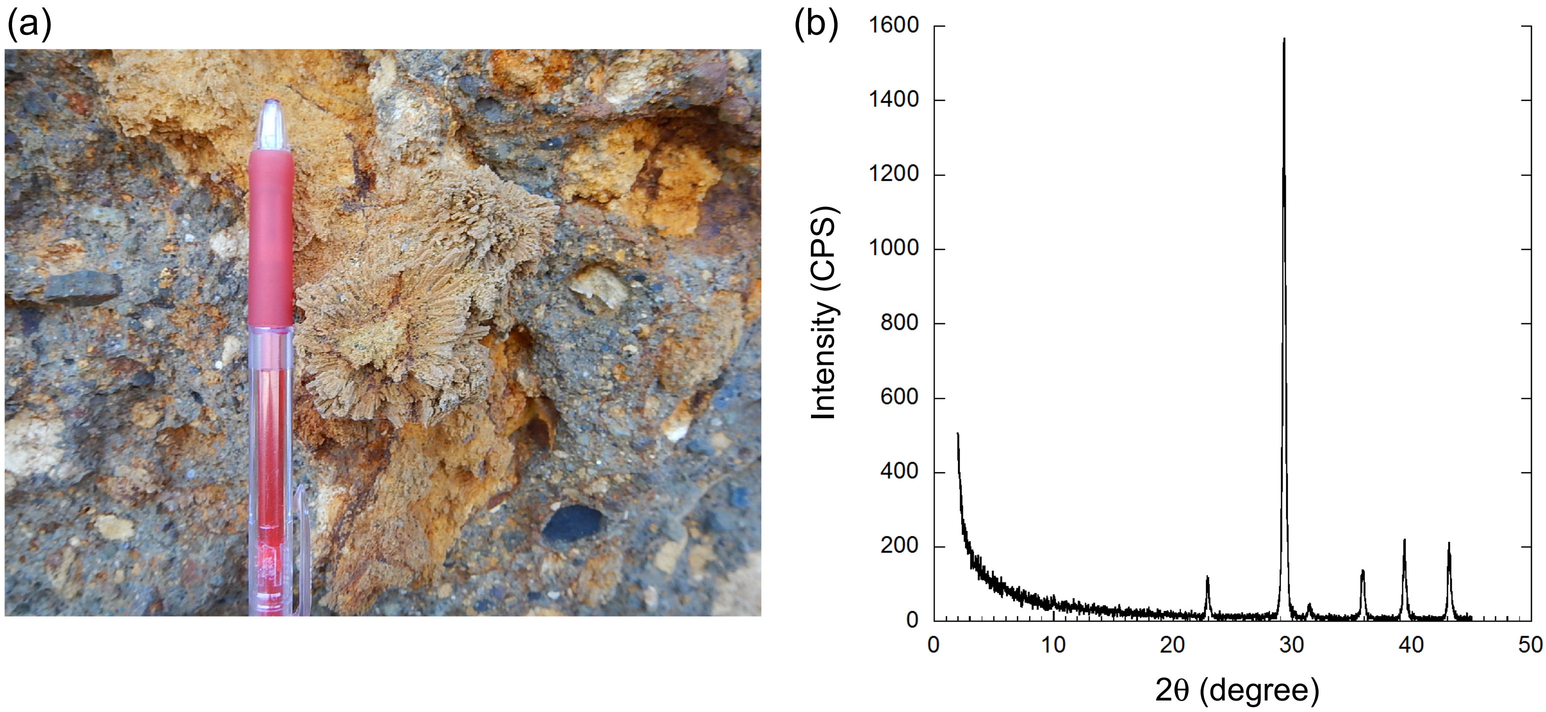
(a)
(b)
Intensity (CPS)
0
200
400
600
800
1000
1200
1400
1600
0
10
20
30
40
50
2θ (degree)

Figure 5

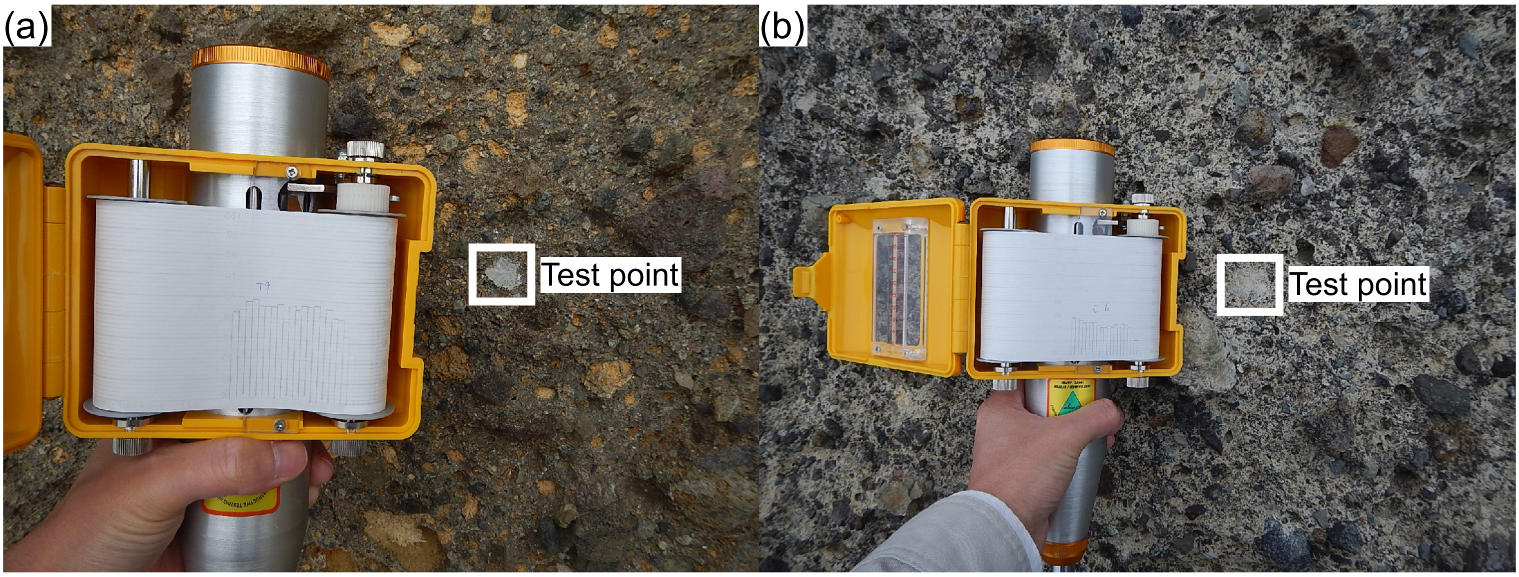

Figure 6

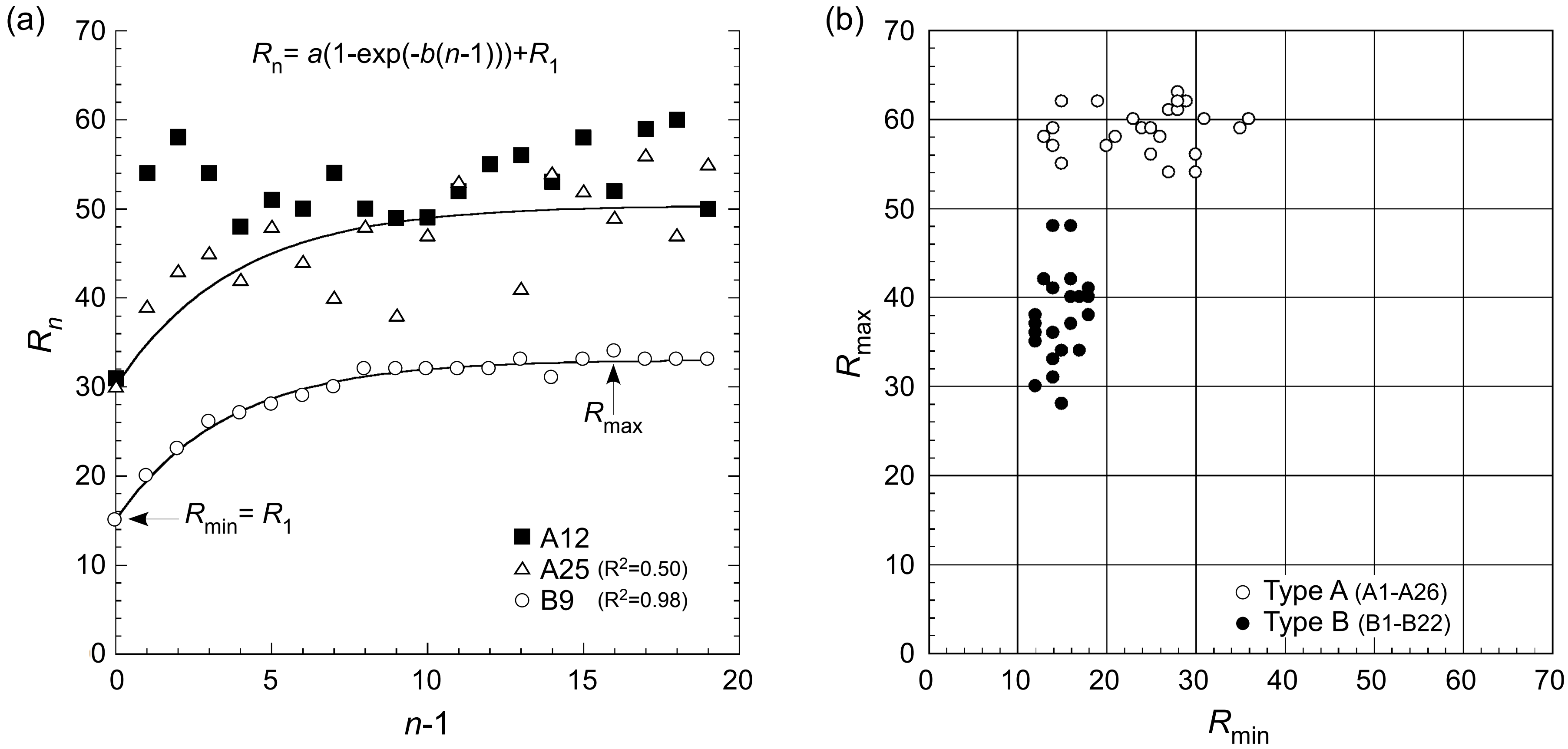

(a)
$R_n = a(1-\exp(-b(n-1)))+R_1$
R_n
n-1
R_{max}
$R_{min} = R_1$
A12
A25 (R^2=0.50)
B9 (R^2=0.98)
(b)
R_{max}
R_{min}
Type A (A1-A26)
Type B (B1-B22)

Figure 7

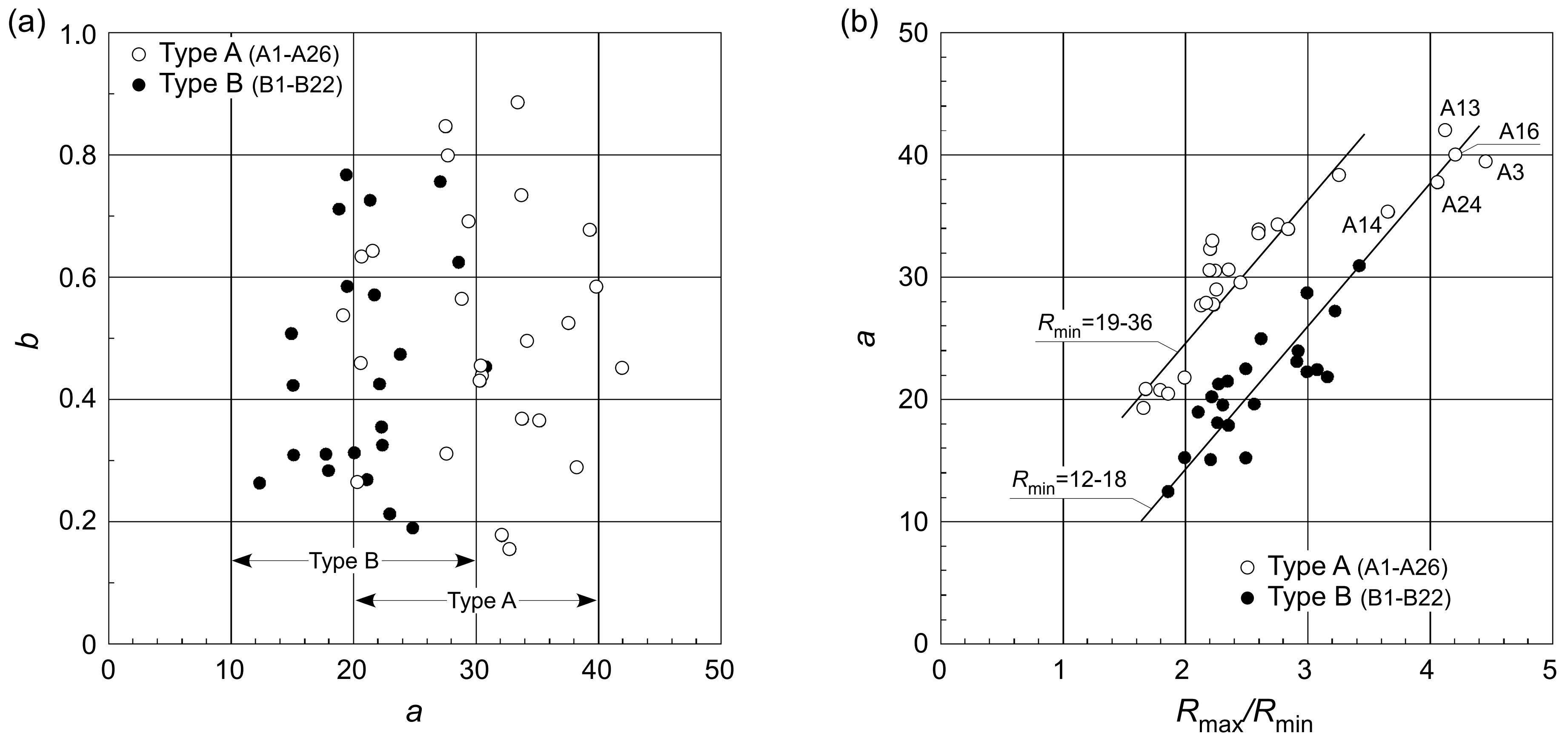
(a)
Type A (A1-A26)
Type B (B1-B22)
b
a
Type B
Type A
(b)
A13
A16
A3
A24
A14
R_{min}=19-36
R_{min}=12-18
Type A (A1-A26)
Type B (B1-B22)
a
R_{max}/R_{min}

Figure 8